Electronic Supplementary Material (ESI) for Journal of Materials Chemistry A.
This journal is © The Royal Society of Chemistry 2014

Electronic Supplementary Information (ESI) for Journal of Materials Chemistry A
This journal is (c) The Royal Society of Chemistry 2014

Supporting Information

Metal-organic frameworks templated nitrogen and sulfur co-doped porous carbons as highly efficient metal-free electrocatalysts for oxygen reduction reaction

Jisen Li,[a,b] Yuyun, Chen,[a] Yujia, Tang,[a] Shunli Li,[a] Huiqing Dong,[a] Kui Li,[a] Min Han,[a] Ya-Qian Lan,[a*] Jianchun Bao[a] and Zhihui Dai[a*]

[a]Jiangsu Key Laboratory of Biofunctional Materials, School of Chemistry and Materials Science
Nanjing Normal University, Nanjing 210023, P. R. China
[b]Department of Chemistry and Chemical Engineering, Jining University, Qufu 273155, P. R. China
*Address correspondence to yqlan@njnu.edu.cn, daizhihuii@njnu.edu.cn

Experimental Sections

Materials and Preparation of the catalysts

All reagents were analytical grade and used without further purification. All solutions used in electrochemical experiments were prepared with Millipore water (≥18 MΩ).

In a typical procedure, 1g MOFs were dried under vacuum at 60 °C for 3 hours and then soaked in a certain amount methanol solution in the presence of urea, or dimethyl sulfoxide (DMSO), or urea and DMSO for about 12 hours. The resulted MOFs were filtered and carbonized in a flow of ultrapure N_2 for 5 hours at 900 °C with the heating rate of 10 °C min^{-1}. The obtained samples were collected and washed with dilute hydrochloric acid solution and distilled water. The co-doped products were dried under vacuum at 60 °C for 5 hours and denoted as NS(A:B)-C-MOF-5 (A:B represents the atomic N:S ratio in NS(A:B)-C-MOF-5, which is listed in Table S1 (ESI†)).

For comparison, the pristine (C-MOF-5) or doped solely carbons with N (N-C-MOF-5) or with S (S-C-MOF-5) were treated under similar conditions.

Characterizations

The HRTEM images were recorded on JEOL-2100F apparatus at an accelerating voltage of 200 kV. Surface morphologies of the carbon materials were examined by a scanning electron microscope (SEM, JSM-7600F) at an acceleration voltage of 10 kV. The EDS spectra were taken on JSM-5160LV-Vantage typed energy spectrometer. The powder X-Ray diffraction (XRD) patterns were recorded on a D/max 2500VL/PC diffractometer (Japan) equipped with graphite monochromatized Cu K_α radiation (λ = 1.54060 Å). Corresponding work voltage and current is 40 kV and 100 mA, respectively. X-ray photon spectroscopy (XPS) was recorded by a scanning X-ray microprobe (PHI 5000 Verasa, ULAC-PHI, Inc.) using Al k_α radiation and the C_{1s} peak at 284.6 eV as internal standard. The Raman spectra of dried samples were obtained on Lab-RAM HR800 with excitation by an argon ion laser (514.5 nm). The nitrogen adsorption-desorption experiments were operated at 77 K on a Micromeritics ASAP 2050 system. Prior to the measurement, the samples were degassed at 150 °C for 10 hours.

Electrode preparation

All electrochemical experiments were conducted on a CHI 760D electrochemical station (Shanghai Chenhua Co., China) in a standard three electrode cell at room temperature. An Ag/AgCl with saturated KCl, and a Pt wire were used as reference and counter electrode, respectively.

The procedures of glass carbon electrodes (5.0 mm in diameter from Gamry Instruments, USA) preparation were as follows: prior to use, the electrodes were polished mechanically with aluminite power under an chamois, successively washed with ethanol and de-ionized water by sonication for 5 minutes, and dried in a desiccator. 4 mg of the catalysts were dispersed in 2 ml of solvent of Nafion (5%) and de-ionized water (1:9) by sonication, respectively. Typically, 10 μl (2 mg/ml) well-dispersed catalysts suspensions were pipetted onto the glassy carbon electrode surface and allowed to dry at room temperature for 30 minutes. For comparison, a commercially available Pt-C (20 wt%, Johnson Matthey) catalyst was prepared in the same way.

Cyclic voltammetry experiments (CVs) were performed at room temperature in 0.1 M KOH solutions which were purged with N_2 or O_2 for at least 30 minutes before measuring oxygen reduction reaction (ORR) activity from -1.0 to 0.2 V at a scan rate of 100 mV s^{-1}.

In the rotating disk electrode (RDE) and rotating ring-disk electrode (RRDE) tests, the linear sweep voltammograms (LSVs) were measured in O_2 saturated 0.1 M KOH solution and the potential was varied from 0.2 to -1.0 V with a scan rate of 10 mV s^{-1} at various rotating speeds from 400 to 1600 rpm.

To examine the ORR performance, the number of electrons (n) was conducted according to Koutecky-Levich (K-L) equation:

(1) $J^{-1} = J_L^{-1} + J_k^{-1} = (B\omega^{1/2})^{-1} + J_k^{-1}$

(2) $B = 0.62nFC_{O2}(D_{O2})^{2/3}\ v^{-1/6}$

(3) $J_k = nFkC_{O2}$

Where J is the measured current density, J_k and J_L are the kinetic and diffusion-limiting current density, respectively. B is Levich slope which is given by (2). N is the number of electrons transferred for ORR. ω is the rotation rate ($\omega = 2\pi N$, N is the linear rotation speed), F is the Faraday constant ($F = 96485$ C mol^{-1}), ν is the kinetic viscosity, and C_{O2} is the concentration of O_2 ($1.2*10^{-3}$ mol L^{-1}), and D_{O2} is the diffusion coefficient of O_2 in 0.1 M KOH ($1.9*10^{-5}$ cm s^{-1}).

The electron transfer numbers (n) were also estimated by the rotating ring-disk electrode (RRDE) technique, which was calculated as follows,

$$n = 4\, I_D / (I_D + I_R / N)$$

where I_D and I_R are the disk current and ring current, respectively, $N = 0.37$ is the current collection efficiency.

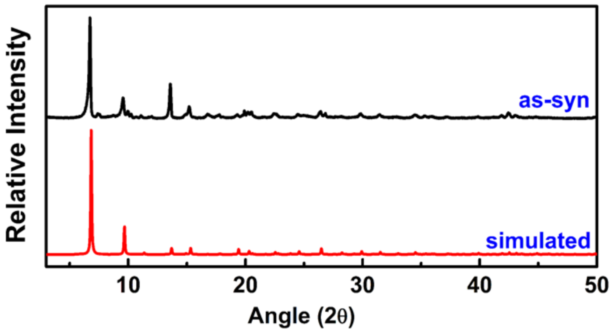

Figure S1. Simulated and synthesized PXRD profiles of MOF-5.

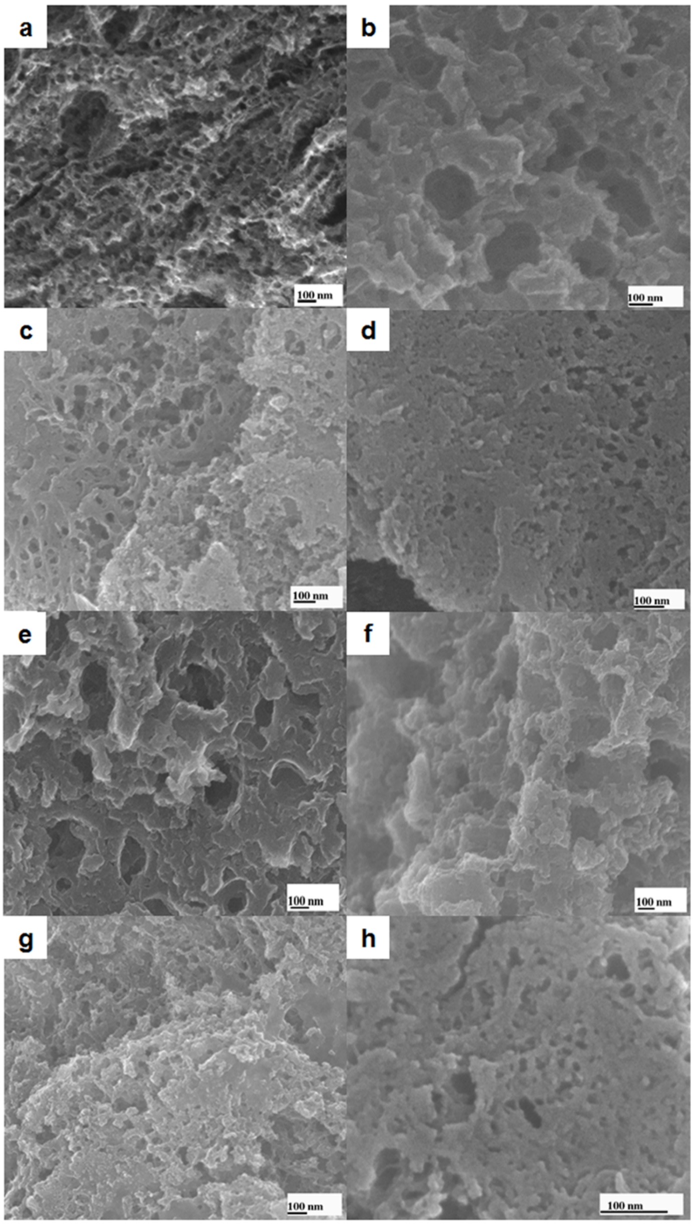

Figure S2. (a-h) SEM of C-MOF-5, S-C-MOF-5, N-C-MOF-5, NS(1:1)-C-MOF-5, NS(1:2)-C-MOF-5, NS(1:3)-C-MOF-5, NS(2:1)-C-MOF-5 and NS(3:1)-C-MOF-5, respectively.

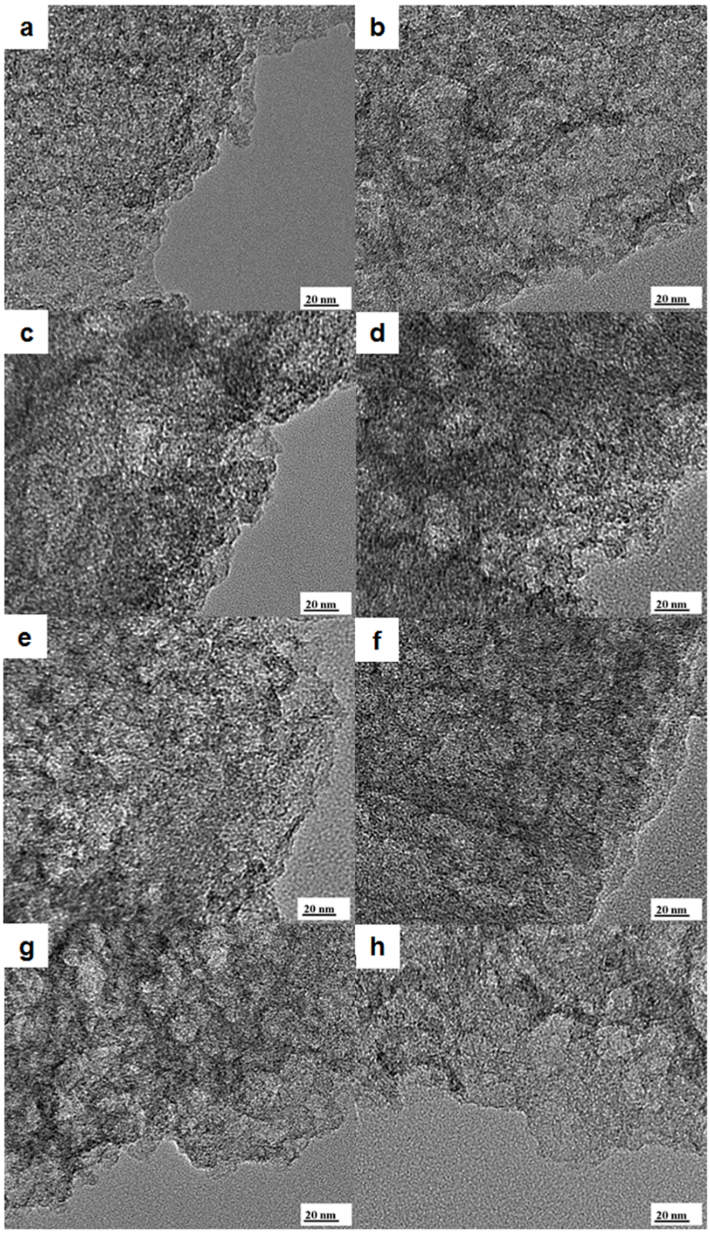

Figure S3. (a-h) HRTEM of C-MOF-5, S-C-MOF-5, N-C-MOF-5, NS(1:1)-C-MOF-5, NS(1:2)-C-MOF-5, NS(1:3)-C-MOF-5, NS(2:1)-C-MOF-5 and NS(3:1)-C-MOF-5, respectively.

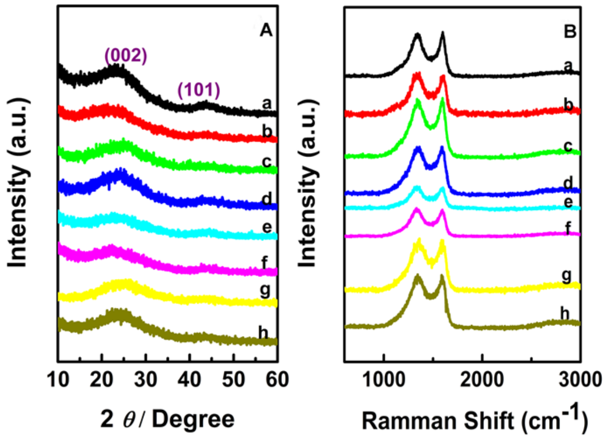

Figure S4. (A) PXRD and (B) Raman spectra curves of (a) C-MOF-5, (b) S-C-MOF-5, (c) N-C-MOF-5, (d) NS(1:1)-C-MOF-5, (e) NS(1:2)-C-MOF-5, (f) NS(1:3)-C-MOF-5, (g) NS(2:1)-C-MOF-5 and (h) NS(3:1)-C-MOF-5, respectively.

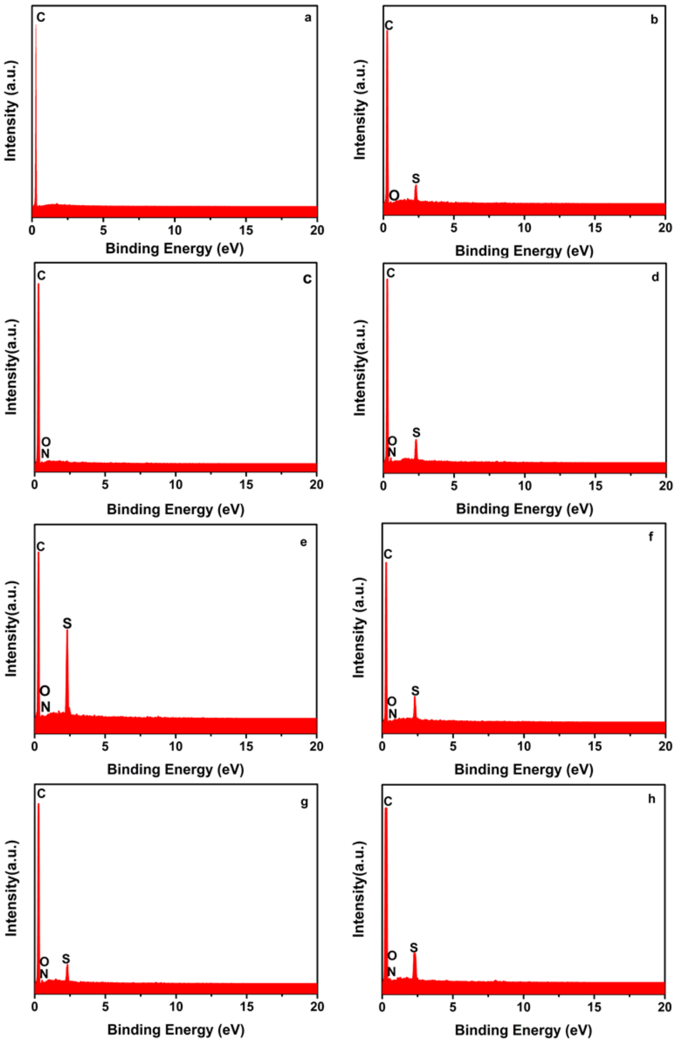

Figure S5. (a-h) EDS of C-MOF-5, S-C-MOF-5, N-C-MOF-5, NS(1:1)-C-MOF-5, NS(1:2)-C-MOF-5, NS(1:3)-C-MOF-5, NS(2:1)-C-MOF-5 and NS(3:1)-C-MOF-5, respectively.

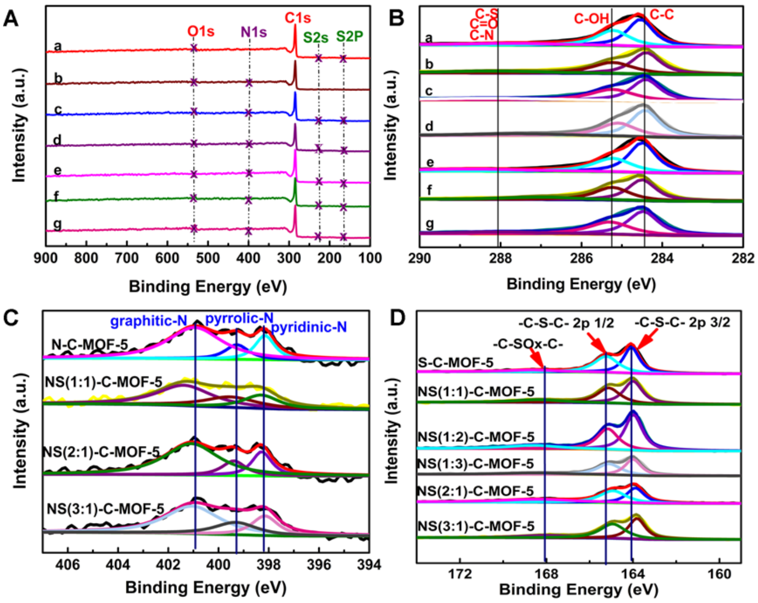

Figure S6. (A) XPS-survey spectra and (B) XPS-C_{1s} spectra of (a) S-C-MOF-5, (b) N-C-MOF-5, (c) NS(1:1)-C-MOF-5, (d) NS(1:2)-C-MOF-5, (e) NS(1:3)-C-MOF-5, (f) NS(2:1)-C-MOF-5 and (g) NS(3:1)-C-MOF-5, respectively. (C) XPS-N_{1s} spectra of N-C-MOF-5 (a), NS(1:1)-C-MOF-5 (b), NS(2:1)-C-MOF-5 (c) and NS(3:1)-C-MOF-5 (d), respectively. (D) XPS-S_{2p} spectra of S-C-MOF-5 (a), NS(1:1)-C-MOF-5 (b), NS(1:2)-C-MOF-5 (c), NS(1:3)-C-MOF-5 (d), NS(2:1)-C-MOF-5 (e) and NS(3:1)-C-MOF-5 (f), respectively. (X: Peak position)

The nature of N or S species in the surface of doped carbons was further investigated by X-ray photoelectron spectroscopy (XPS) technique (Fig. S6A). The high resolution of C_{1s} spectra of the doped porous carbons indicate that the peaks at 284.5 eV correspond to the sp^2 hybridized C=C bonds which indicate that graphite carbons are the majority, while the peaks at about 285.5 eV confirm the present of C-O, C-S and C-N,[31] and the peaks around 288.1 eV are assigned to C=O configurations (Fig. S6).[7] As illustrated in Fig. S6C, the N_{1s} XPS spectra of N doped carbon materials can be fitted into three peaks at about 400.9, 399.8 and 398.6 eV, respectively.[7] The peaks are assigned to graphitic N (~ 400.9 eV), prrolic N (~399.8 eV) and pyridinic N (~398.6 eV), respectively. From Fig. S6C, it can be found that graphitic and pyridinic nitrogen of the N doped carbon materials are the main components, compared to pyrrolic nitrogen. It is advantageous for the metal-free carbon materials to be used for ORR, as the graphitic and pyridinic groups have been shown to be more active than their pyrrolic counterpart. On the other hand, the binding energy of XPS-S_{2p} is used to analyze the elemental sulfur in the case of S-C-MOF-5 catalyst and NS(A:B)-C-MOF-5 catalyst. As shown in Fig. S6D , two peaks appear at approximately 163.9 and 165.0 eV, which are assigned to $S_{2p\ 3/2}$ and $S_{2p\ 1/2}$, respectively, as the dominant products; the weak peak at about 168.5 eV is attributed to oxidized sulfur groups (-C-SOx-C-),[18] which are unconspicuous and chemically inactive for ORR.

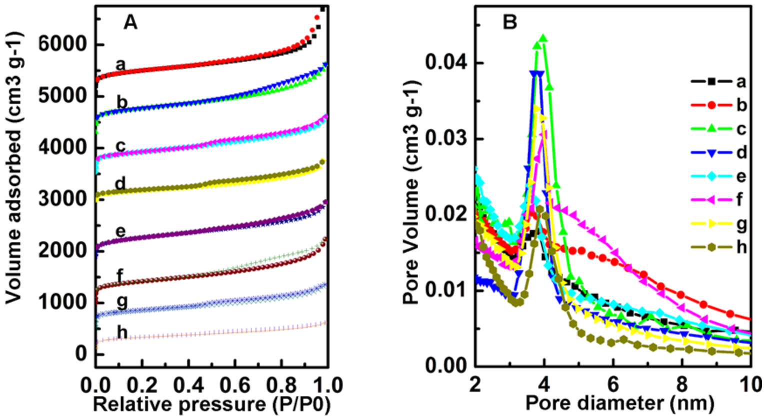

Figure S7. (A) N_2 adsorption-desorption isotherms and (B) pore size distributions of C-MOF-5 (a), S-C-MOF-5 (b), N-C-MOF-5 (c), NS(1:1)-C-MOF-5 (d), NS(1:2)-C-MOF-5 (e), NS(1:3)-C-MOF-5 (f), NS(2:1)-C-MOF-5 (g) and NS(3:1)-C-MOF-5 (h), respectively.

The nitrogen adsorption-desorption isotherms of all carbon materials are of type IV with distinct hysteresis loops (Fig. S7A). The average pore size of all the samples is about 3.8 nm by BJH model according to the desorption branch (Fig. S7B), which is characteristic of mesopores. In terms of the mesopore, it is beneficial to facilitate the diffusion of reactants for ORR.[13, 18]

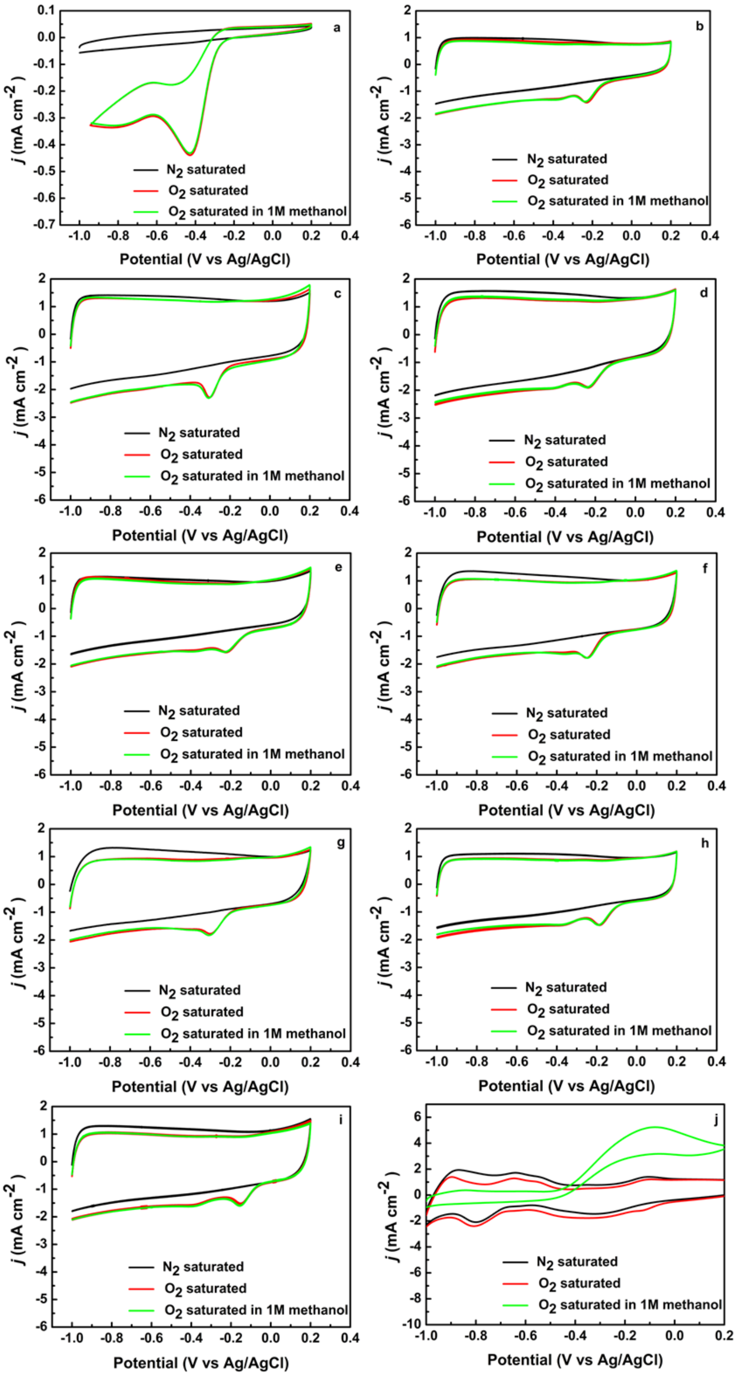

Figure S8. (a-j) CVs of BGC, C-MOF-5, S-C-MOF-5, N-C-MOF-5, NS(1:1)-C-MOF-5, NS(1:2)-C-MOF-5, NS(1:3)-C-MOF-5, NS(2:1)-C-MOF-5, NS(3:1)-C-MOF-5 and Pt-C electrodes in an aqueous solution of 0.1 M KOH saturated by N_2 or O_2 or O_2-saturated 0.1 M solution of KOH solution upon addition of methanol for the ORR.

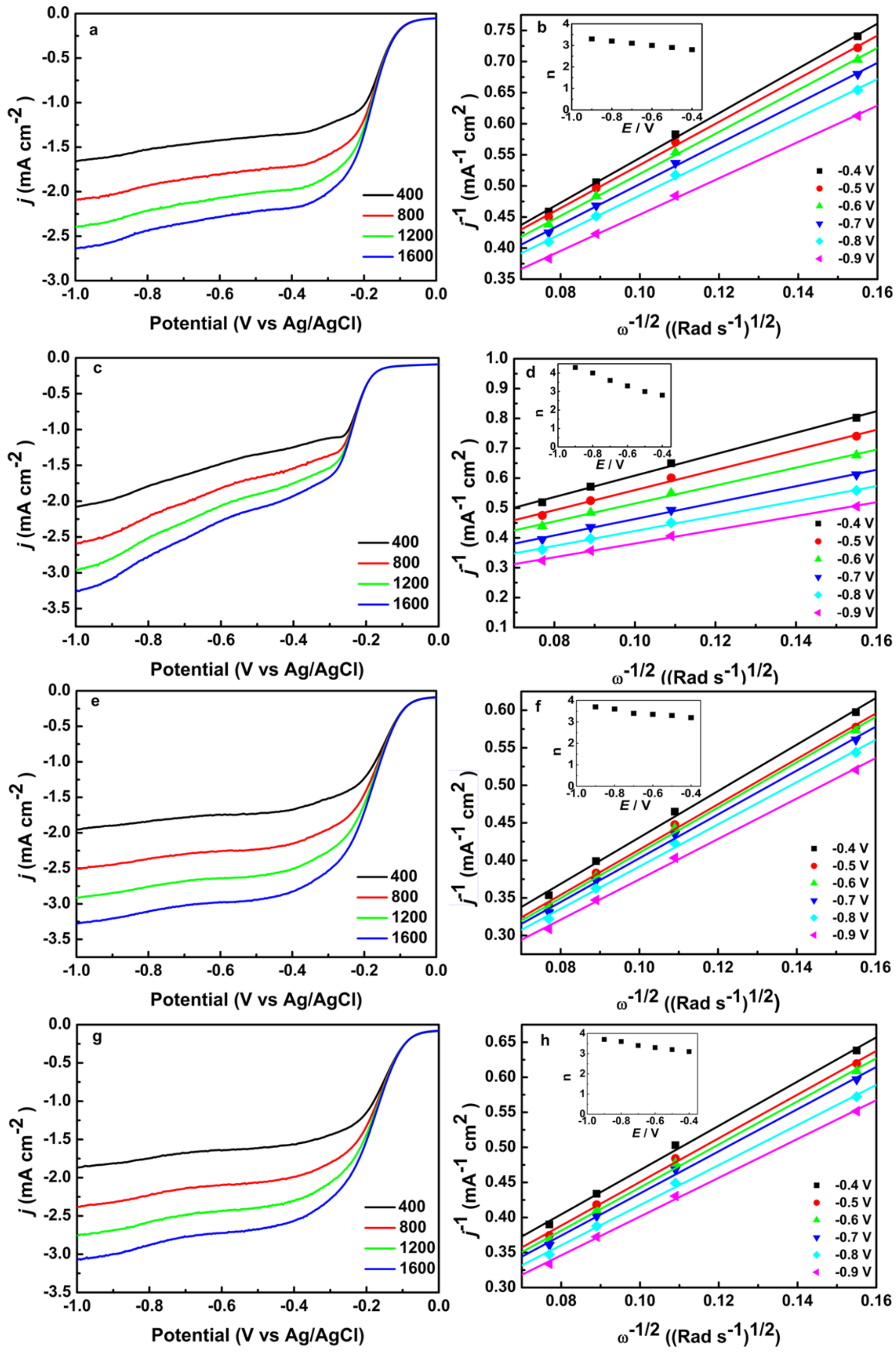
a
b
c
d
e
f
g
h
400
800
1200
1600
-0.4 V
-0.5 V
-0.6 V
-0.7 V
-0.8 V
-0.9 V
j (mA cm-2)
Potential (V vs Ag/AgCl)
j-1 (mA-1 cm2)
ω-1/2 ((Rad s-1)1/2)
n
E / V

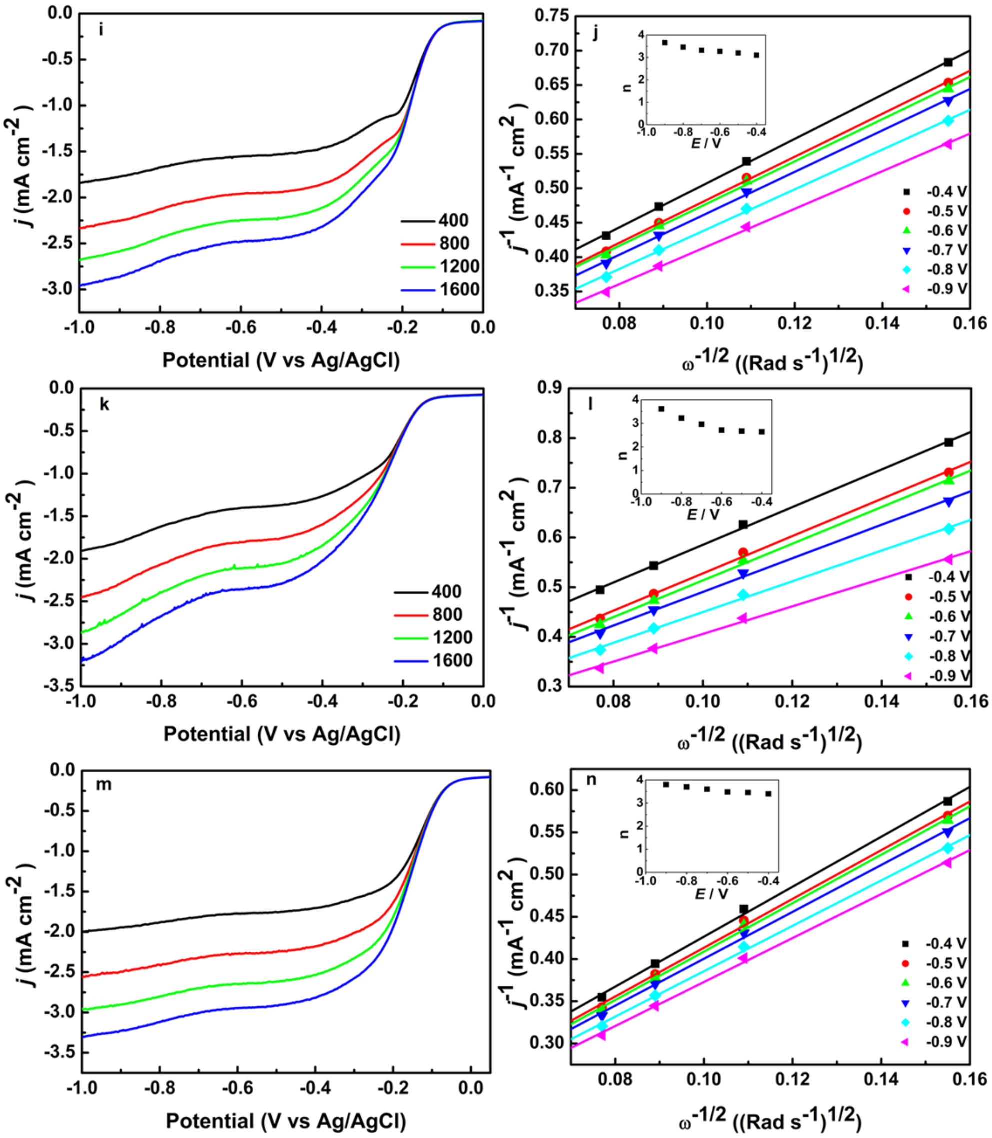

Figure S9. LSVs and K-L plots of C-MOF-5 (a, b), S-C-MOF-5 (c, d), N-C-MOF-5 (e, f), NS(1:1)-C-MOF-5 (g, h), NS(1:2)-C-MOF-5 (i, j), NS(1:3)-C-MOF-5 (k, l) and NS(2:1)-MOF-5 (m, n) in O_2-satureated 0.1 M KOH solution with a sweep rate of 10 mV s^{-1} from -0.4 to -0.9 V, respectively. The inset shows the dependence of n on the potential on the corresponding left.

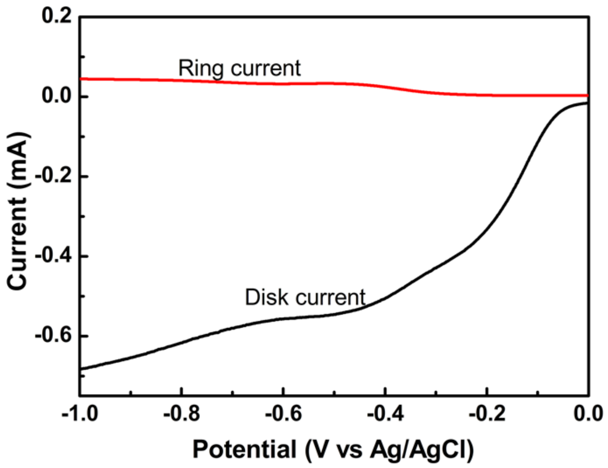

Figure S10. RRDE voltammograms of the NS(3:1)-C-MOF-5 electrode in an O_2-saturated 0.1 M KOH solution at a scan rate of 10 mV s^{-1} and a rotating rate of 1600 rpm, and the ring potential is kept constant at 0.5 V versus Ag/AgCl.

To further examine the ORR catalytic pathways of NS(3:1)-C-MOF-5, we carried out rotating ring-disk electrode (RRDE) measurement. The average electron transfer number of the NS(3:1)-C-MOF-5 catalyst is about 3.6.

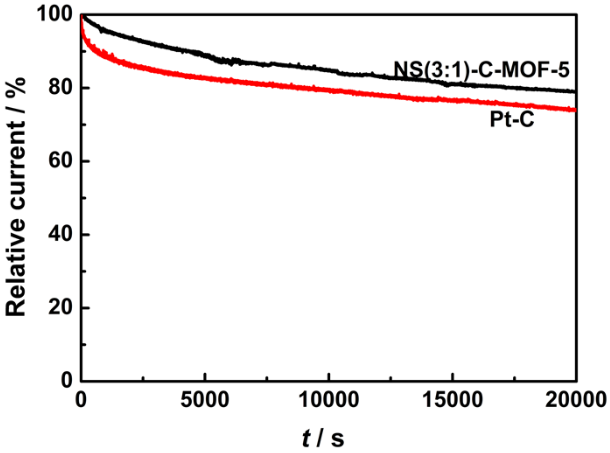

Figure S11. Current-time (i-t) chronoamperometric response of NS(3:1)-C-MOF-5 and Pt-C electrodes at -0.4 V in O_2-saturated 0.1 M KOH at a rotation rate of 1600 rpm.

Table S1 Elemental compositions of the porous carbon materials after carbonization at 900 °C, determined by XPS on the left. The BET surface areas of the porous carbon materials are shown on the right.

	Elemental composition (at %)				**BET surface**
Materials	C	N	S	about atomic N:S ratio	**area (m^2 g^{-1})**
C-MOF-5	95.83	—[a]	—[a]	—[a]	1673
S-C-MOF-5	93.54	—[a]	2.3	—[a]	1588
N-C-MOF-5	92.9	3.65	—[a]	—[a]	1466
NS(1:1)-C-MOF-5	90.3	1.31	1.21	1:1	942
NS(1:2)-C-MOF-5	93	0.69	1.52	1:2	1577
NS(1:3)-C-MOF-5	95.52	0.61	1.79	1:3	1421
NS(2:1)-C-MOF-5	90.9	2.31	1.14	2:1	1195
NS(3:1)-C-MOF-5	88.85	3.31	1.08	3:1	1091

[a] No available data for the comparisons.

Table S2 Comparisons of electrochemical properties for different carbons at various conditions.

	Materials	**Reference electrode**	**Peak potential(V)**	**Onset potential(V)**	**Electrolyte**	**Refs.**
	NS(3:1)-C-MOF-5	**NHE**	**0.047**	**0.192**	**0.1 M KOH**	**This work**
	NS(2:1)-C-MOF-5	**NHE**	**-0.003**	**0.187**	**0.1 M KOH**	**This work**
	NS(1:1)-C-MOF-5	**NHE**	**-0.013**	**0.177**	**0.1 M KOH**	**This work**
	NS(1:2)-C-MOF-5	**NHE**	**-0.053**	**0.137**	**0.1 M KOH**	**This work**
	NS(1:3)-C-MOF-5	**NHE**	**-0.093**	**0.107**	**0.1 M KOH**	**This work**
	N-C-MOF-5	**NHE**	**-0.033**	**0.174**	**0.1 M KOH**	**This work**
	S-C-MOF-5	**NHE**	**-0.103**	**0.087**	**0.1 M KOH**	**This work**
	C-MOF-5	**NHE**	**-0.043**	**0.167**	**0.1 M KOH**	**This work**
N-doped	**N-C-MOF-5**	**NHE**	**-0.033**	**0.174**	**0.1 M KOH**	**This work**
	B_3CNTs	NHE	-0.108[a]	-0.008[b]	1.0 M NaOH	1
	B_3CNTs-NH_3	NHE	-0.068[a]	0.022[b]	1.0 M NaOH	2
	N-graphene	NHE	-0.165[b]	0.025[b]	0.1 M KOH	3

	NCNTs (BTA)	NHE	-0.009[a]	-0.079[a]	0.1 M KOH	4
	VA-BCN	NHE	-0.058[b]	0.092[b]	0.1 M KOH	5
	PDDA-graphene	NHE	-0.108[a]	0.092[a]	0.1 M KOH	6
	NG-NCNT	NHE	-0.058[b]	0.102[a]	0.1 M KOH	7
	NOMGAs	NHE	-0.055[a]	0.075[a]	0.1 M KOH	8
	N-graphene	NHE	-0.115[b]	0.075[a]	0.1 M KOH	9
	NCNTs	NHE	-0.073[a]	0.077[b]	0.1 M KOH	10
	N-graphene	NHE	-0.023[a]	0.077[b]	0.1 M KOH	11
	NG5	NHE	-0.103[b]	0.097[a]	0.1 M KOH	12
	G–CN800	NHE	-0.045[a]	0.105[b]	0.1 M KOH	13
	g-C_3N_4@CMK-3	NHE	0.017[a]	0.097[a]	0.1 M KOH	14
	PDDA-ACNT	NHE	-0.038[a]	0.152[a]	0.1 M KOH	15
	VA-NCNT	NHE	0.047[a]	0.117[a]	0.1 M KOH	16
	N-HCNPs	NHE	-0.095[a]	0.125[a]	0.1 M KOH	17
	NG	NHE	-0.115[a]	0.165[a]	0.1 M KOH	18
	N-RG-O (850℃)	NHE	—[c]	0.167[b]	0.1 M KOH	19
	NG-900	NHE	0.045[a]	0.175[a]	0.1 M KOH	20
	BCN-graphene	NHE	-0.038[a]	0.242[b]	0.1 M KOH	21
	MNC-800	NHE	0.025[b]	0.235[a]	1.0 M NaOH	22
	Meso-EmG	NHE	0.005[a]	0.232[a]	0.1 M KOH	23
	NCNT-1000	NHE	-0.095[a]	0.325[a]	0.1 M KOH	24
	N-graphene (900)	NHE	-0.05[b]	0.308[a]	0.1 M KOH	25
S-doped	**S-C-MOF-5**	**NHE**	**-0.103**	**0.087**	**0.1 M KOH**	**This work**
	SGnP	NHE	-0.145[b]	0.045[a]	0.1 M KOH	26
	S-graphene-1050	NHE	-0.093[b]	0.117[b]	0.1 M KOH	27
	SGnP	NHE	-0.195[a]	-0.015[a]	0.1 M KOH	28
N and S co-doped	**NS(3:1)-C-MOF-5**	**NHE**	**0.047**	**0.192**	**0.1 M KOH**	**This work**
	NS(2:1)-C-MOF-5	**NHE**	**-0.003**	**0.187**	**0.1 M KOH**	**This work**

NS(1:1)-C-MOF-5	**NHE**	**-0.013**	**0.177**	**0.1 M KOH**	**This work**
NS(1:2)-C-MOF-5	**NHE**	**-0.053**	**0.137**	**0.1 M KOH**	**This work**
NS(1:3)-C-MOF-5	**NHE**	**-0.093**	**0.107**	**0.1 M KOH**	**This work**
CA-TCA_900	NHE	-0.153[a]	0.067[a]	0.1 M KOH	29
SNGL-20	NHE	0.017[a]	0.087[a]	0.1 M NaOH	30
N-S-graphene	NHE	-0.035[a]	0.145[b]	0.1 M KOH	31

[a] Reported values derived from the ref.

[b] Reported values estimated from the ref.

[c] No data derived from the ref.

References:

1. L. Yang, S. Jiang, Y. Zhao, L. Zhu, S. Chen, X. Wang, Q. Wu, J. Ma, Y. Ma and Z. Hu, *Angew. Chem. Int. Ed.*, 2011, **50**, 7132.

2. Y. Zhao, L. Yang, S. Chen, X. Wang, Y. Ma, Q. Wu, Y. Jiang, W. Qian and Z. Hu, *J. Am. Chem. Soc.*, 2013, **135**, 1201.

3. L. Qu, Y. Liu, J.-B. Baek and L. Dai, *ACS nano*, 2010, **4**, 1321.

4. A. Morozan, P. Jegou, M. Pinault, S. Campidelli, B. Jousselme and S. Palacin, *ChemSusChem*, 2012, **5**, 647.

5. S. Wang, E. Iyyamperumal, A. Roy, Y. Xue, D. Yu and L. Dai, *Angew. Chem. Int. Ed.*, 2011, **50**, 11756.

6. S. Wang, D. Yu, L. Dai, D. W. Chang and J.-B. Baek, *ACS nano*, 2011, **5**, 6202.

7. P. Chen, T.-Y. Xiao, Y.-H. Qian, S.-S. Li and S.-H. Yu, *Adv. Mater.*, 2013, **25**, 3192.

8. R. Liu, D. Wu, X. Feng and K. Müllen, *Angew. Chem. Int. Ed.*, 2010, 49, 2565.

9. I.-Y. Jeon, D. Yu, S.-Y. Bae, H.-J. Choi, D. W. Chang, L. Dai and J.-B. Baek, *Chem. Mater.*, 2011, **23**, 3987.

10. Z. Wang, R. Jia, J. Zheng, J. Zhao, L. Li, J. Song and Z. Zhu, *ACS nano*, 2011, **5**, 1677.

11. Z. Lin, G. H. Waller, Y. Liu, M. Liu and C.-p. Wong, *Carbon*, 2013, **53**, 130.

12. Z.-H. Sheng, L. Shao, J.-J. Chen, W.-J. Bao, F.-B. Wang and X.-H. Xia, *ACS nano*, 2011, **5**, 4350.

13. S. Yang, X. Feng, X. Wang and K. Müllen, *Angew. Chem. Int. Ed.*, 2011, **50**, 5339.

14. Y. Zheng, Y. Jiao, J. Chen, J. Liu, J. Liang, A. Du, W. Zhang, Z. Zhu, S. C. Smith, M. Jaroniec, G. Q. Lu and S. Z. Qiao, *J. Am. Chem. Soc.*, 2011, **133**, 20116.

15. S. Y. Wang, D. S. Yu and L. M. Dai, *J. Am. Chem. Soc.*, 2011, **133**, 5182.

16. K. P. Gong, F. Du, Z. H. Xia, M. Durstock and L. M. Dai, *Science*, 2009, **323**, 760.

17. G. Ma, R. Jia, J. Zhao, Z. Wang, C. Song, S. Jia and Z. Zhu, *J. Phys. Chem. C*, 2011, **115**, 25148.

18. S. Yang, L. Zhi, K. Tang, X. Feng, J. Maier and K. Müllen, *Adv. Func. Mater.*, 2012, **22**, 3634.

19. L. Lai, J. R. Potts, D. Zhan, L. Wang, C. K. Poh, C. Tang, H. Gong, Z. Shen, J. Lin and R. S. Ruoff, *Energy Environ. Sci.*, 2012, **5**, 7936.

20. K. Parvez, S. B. Yang, Y. Hernandez, A. Winter, A. Turchanin, X. L. Feng and K. Müllen, *ACS nano*, 2012, **6**, 9541.

21. S. Wang, L. Zhang, Z. Xia, A. Roy, D. W. Chang, J. B. Baek, and L. Dai, *Angew. Chem. Int. Ed*. 2012, **51**, 4209.

22. T. C. Nagaiah, A. Bordoloi, M. D. Sanchez, M. Muhler and W. Schuhmann, *ChemSusChem*, 2012, **5**, 637.

23. W. Yang, T. P. Fellinger and M. Antonietti, *J. Am. Chem. Soc.*, 2011, **133**, 206.

24. T. Sharifi, G. Hu, X. Jia and T. Wagberg, *ACS nano*, 2012, **6**, 8904.

25. D. Geng, Y. Chen, Y. Chen, Y. Li, R. Li, X. Sun, S. Ye and S. Knights, *Energy Environ. Sci.*, 2011, **4**, 760.

26. I. Y. Jeon, H. J. Choi, S. M. Jung, J. M. Seo, M. J. Kim, L. Dai and J. B. Baek, *J. Am. Chem. Soc.*, 2013, **135**, 1386.

27. Z. Yang, Z. Yao, G. Li, G. Fang, H. Nie, Z. Liu, X. Zhou, X. Chen and S. Huang, *ACS nano*, 2012, **6**, 205.

28. I. Y. Jeon, S. Zhang, L. Zhang, H. J. Choi, J. M. Seo, Z. Xia, L. Dai and J. B. Baek, *Adv. Mater*., 2013. DOI: 10.1002/adma201302753.

29. S. A. Wohlgemuth, R. J. White, M. G. Willinger, M. M. Titirici and M. Antonietti, *Green Chem*., 2012, **14**, 1515.

30. J. Xu, G. Dong, C. Jin, M. Huang and L. Guan, *ChemSusChem*, 2013, **6**, 493.

31. J. Liang, Y. Jiao, M. Jaroniec, S. Z. Qiao, J. Liang, Y. Jiao, M. Jaroniec and S. Z. Qiao, *Angew. Chem. Int. Ed*., 2012, **51**, 11496.